

This discussion paper is/has been under review for the journal *Atmospheric Chemistry and Physics (ACP)*. Please refer to the corresponding final paper in *ACP* if available.

**EPP in EMAC, NO_x
downward transport**

A. J. G. Baumgaertner
et al.

Energetic particle precipitation in ECHAM5/MESSy1 – Part 1: Downward transport of upper atmospheric NO_x produced by low energy electrons

A. J. G. Baumgaertner, P. Jöckel, and C. Brühl

Max Planck Institute for Chemistry, Mainz, Germany

Received: 2 October 2008 – Accepted: 21 October 2008 – Published: 18 December 2008

Correspondence to: A. J. G. Baumgaertner (abaumg@mpch-mainz.mpg.de)

Published by Copernicus Publications on behalf of the European Geosciences Union.

Title Page

Abstract

Introduction

Conclusions

References

Tables

Figures

◀

▶

◀

▶

Back

Close

Full Screen / Esc

Printer-friendly Version

Interactive Discussion



Abstract

The atmospheric chemistry general circulation model ECHAM5/MESSy1 has been extended by processes that parameterize particle precipitation. Several types of particle precipitation that directly affect NO_y and HO_x concentrations in the middle atmosphere are accounted for and discussed in a series of papers. In the companion paper, the ECHAM5/MESSy1 solar proton event parameterization is discussed, while in the current paper we focus on low energy electrons (LEE) that produce NO_x in the upper atmosphere. For the flux of LEE NO_x into the top of the model domain a novel technique which can be applied to most atmospheric chemistry general circulation models has been developed and is presented here. The technique is particularly useful for models with an upper boundary between the stratopause and mesopause and therefore cannot directly incorporate upper atmospheric NO_x production. The additional NO_x source parametrization is based on a measure of geomagnetic activity, the A_p index, which has been shown to be a good proxy for LEE NO_x interannual variations. HALOE measurements of LEE NO_x that has been transported into the stratosphere are used to develop a scaling function which yields a flux of NO_x that is applied to the model top. We describe the implementation of the parameterization as the sub-model SPACENOX in ECHAM5/MESSy1 and discuss the results from test simulations. The NO_x enhancements and associated effects on ozone are shown to be in good agreement with independent measurements. A_p index data is available for almost one century, thus the parameterization is suitable for simulations of the recent climate.

1 Introduction

Since the 1980's measurements and models have shown that under certain circumstances, NO_x produced in the thermosphere by precipitating low energy electrons (LEE) can be transported downward into the stratosphere and there engage in catalytic ozone destruction. There is emerging evidence that this is an important process

ACPD

8, 21201–21228, 2008

EPP in EMAC, NO_x downward transport

A. J. G. Baumgaertner
et al.

Title Page

Abstract

Introduction

Conclusions

References

Tables

Figures

◀

▶

◀

▶

Back

Close

Full Screen / Esc

Printer-friendly Version

Interactive Discussion



**EPP in EMAC, NO_x
downward transport**A. J. G. Baumgaertner
et al.

amongst several sun-earth connection mechanisms (e.g. Rozanov et al., 2005). The electrons with energies between approximately 50 and 1000 eV originate at the sun and from magnetospheric reservoirs, and precipitate at high latitudes during times of enhanced geomagnetic activity. There they lead to the production of NO_x through dissociation and ionization processes (Rusch et al., 1981). In the polar winter, where the photochemical loss of NO_x is negligible and where the Brewer-Dobson circulation leads to a downward transport, NO_x enhancements can be transported down into the stratosphere and lead to significant ozone loss. This has been termed the energetic particle precipitation (EPP) indirect effect, in contrast to the EPP direct effect where NO_x and HO_x is produced in the middle atmosphere mainly through highly energetic electrons and protons.

Measurements of enhancements of NO_x formed by low energy electrons (LEE NO_x) have been made by a growing number of instruments. The Limb Infrared Monitor of the Stratosphere (LIMS) observed NO₂ mixing ratios of up to 175 ppbv in the 1978/1979 winter (Russell et al., 1988). The fact that such enhancements of NO_x occur on a regular basis was realized when Halogen Occultation Experiment (HALOE) data became available. Such observations are for example described in Siskind et al. (2000), Hood and Soukharev (2006) and Randall et al. (2007). Other studies of this type include Randall et al. (1998) which showed NO₂ enhancements using the Polar Ozone and Aerosol Measurement (POAM II) instrument and Rinsland et al. (1999) which reported polar winter NO_y descent seen by the Atmospheric Trace Molecule Spectroscopy (ATMOS) spectrometer on board the space shuttle.

An extensive study using the Michelson Interferometer for Passive Atmospheric Sounding (MIPAS) on board ENVISAT by Funke et al. (2005) clearly showed NO_x enhancements in the 2003 Southern Hemisphere winter stratosphere with mixing ratios up to 200 ppbv. Seppälä et al. (2007) used GOMOS and POAM III measurements to show that the descent of LEE NO_x can be a major contributor to stratospheric NO_x enhancements also in the Northern Hemisphere.

Only recently studies have been able to argue conclusively that stratospheric NO_x

[Title Page](#)[Abstract](#)[Introduction](#)[Conclusions](#)[References](#)[Tables](#)[Figures](#)[◀](#)[▶](#)[◀](#)[▶](#)[Back](#)[Close](#)[Full Screen / Esc](#)[Printer-friendly Version](#)[Interactive Discussion](#)

enhancements due to LEE are linked to geomagnetic activity. Such results are for example presented in Siskind et al. (2000), Hood and Soukharev (2006), and Randall et al. (2007). As a measure for general global geomagnetic activity often the A_p index is employed. The A_p index is derived from magnetic field component measurements at 13 subauroral geomagnetic observatories (Mayaud, 1980).

Treatment of an additional NO_x source in the mesosphere and thermosphere in models has been neglected apart from very few sensitivity studies. Siskind et al. (1997) used a two-dimensional chemical transport model which included E-region chemistry and an ionization source due to auroral particles. However, problems with the model dynamics prevented a good agreement with HALOE data. A very recent study by Vogel et al. (2008) studied Arctic Winter 2003/04 ozone loss resulting from mesospheric NO_x . The CLaMS model in combination with MIPAS satellite data were employed and a significant impact on stratospheric ozone as well as on total column ozone were found. An idealized NO_x source in the upper mesosphere representing relativistic electron precipitation (REP) was implemented into the Freie Universität Berlin Climate Middle Atmosphere Model with online chemistry (FUB-CMAM-CHEM) by Langematz et al. (2005). Although the source was likely to be overestimated, the results showed that the mechanism is important for ozone chemistry. A positive response was reported for ozone at high latitudes at 40–45 km, and a negative response for the tropical lower stratosphere.

Here, we describe a simple parameterization for NO_x produced by LEE for use in atmospheric chemistry general circulation models (AC-GCMs). The combination of the Modular Earth Submodel System (MESSy) and the general circulation model ECHAM5 is briefly introduced in Sect. 2.1. Due to the fact that the upper boundary of ECHAM/MESSy (EMAC) in the MA setup is located at 0.01 hPa, the AC-GCM is well suited for this study. The parameterization and its implementation in EMAC in form of the submodel SPACENOX are described in Sect. 2.2. The validation and the discussion of the results is presented in Sect. 3.

EPP in EMAC, NO_x downward transportA. J. G. Baumgaertner
et al.[Title Page](#)[Abstract](#)[Introduction](#)[Conclusions](#)[References](#)[Tables](#)[Figures](#)[◀](#)[▶](#)[◀](#)[▶](#)[Back](#)[Close](#)[Full Screen / Esc](#)[Printer-friendly Version](#)[Interactive Discussion](#)

2 Model description

2.1 ECHAM5/MESSy1

The ECHAM/MESSy Atmospheric Chemistry (EMAC) model is a numerical chemistry and climate simulation system that includes submodels describing tropospheric and middle atmosphere processes and their interaction with oceans, land and human influences (Jöckel et al., 2006). It uses the first version of the Modular Earth Submodel System (MESSy1) to link multi-institutional computer codes. The core atmospheric model is the 5th generation European Centre Hamburg general circulation model (ECHAM5, Roeckner et al., 2006). The model has been shown to consistently simulate key atmospheric tracers such as ozone (Jöckel et al., 2006), water vapour (Lelieveld et al., 2007), and lower and middle stratospheric NO_y (Brühl et al., 2007). For the present study we applied EMAC (ECHAM5 version 5.3.01, MESSy version 1.6) in the T42L90MA-resolution, i.e. with a spherical truncation of T42 (corresponding to a quadratic gaussian grid of approx. 2.8 by 2.8 degrees in latitude and longitude) with 90 vertical hybrid pressure levels up to 0.01 hPa. This part of the setup matches the model evaluation study by Jöckel et al. (2006). Enabled submodels are also the same as in Jöckel et al. (2006) apart from the new submodels SPE and SPACENOX, a more detailed treatment of the solar variation in the photolysis submodel JVAL, and the sub-submodel FUBRad (Nissen et al., 2007), a high-resolution short-wave heating rate parameterization. The submodel SPE is described in the companion paper Baumgaertner et al. (2008), SPACENOX is described here. The chosen chemistry scheme for the configuration of the submodel MECCA1 (Sander et al., 2005) is simpler compared to the configuration in Jöckel et al. (2006). For example, the NMHC chemistry is not treated at the same level of detail. The complete mechanism is documented in the supplement (<http://www.atmos-chem-phys-discuss.net/8/21201/2008/acpd-8-21201-2008-supplement.zip>).

EPP in EMAC, NO_x downward transport

A. J. G. Baumgaertner
et al.

Title Page

Abstract

Introduction

Conclusions

References

Tables

Figures

◀

▶

◀

▶

Back

Close

Full Screen / Esc

Printer-friendly Version

Interactive Discussion



2.2 The submodel SPACENOX

The focus of this work is to study the interannual variability of LEE NO_x and its temporal and spatial behavior during the polar winter. Randall et al. (1998) and Siskind et al. (2000) have shown that the A_p index is in general sufficient to describe measured interannual variations in the polar vortex. Therefore, the A_p index was chosen as the only required time-varying input for the parameterization. In order to obtain the measured NO_x mixing ratios in the model stratosphere, the A_p index needs to be scaled appropriately to yield the required NO_x flux at the model top. Estimates of NO_x produced in the thermosphere and transported downward into the southern polar stratosphere have been derived from HALOE measurements by Randall et al. (2007), hereafter referred to as R07. Their results cover the years 1992 to 2005 and thus cover more than one solar cycle. This is probably the longest time series of such measurements available. It encompasses the entire spectrum of geomagnetic activity and the A_p index, which has been shown to have a superimposed variation of the time scale of the length of the solar cycle.

In order to develop a scaling function for the flux at the model top, the A_p index was averaged over the period from May to July to yield annual mean values. This time series was fitted to the amount of average annual excess NO_x at 45 km presented in R07 (their Fig. 9) using a least squares fitting algorithm. This yields the function

$$f_{\text{LEE-NOX}}(A_p) = A_p^{2.5} \cdot 1.04 \times 10^3 \cdot 1 \text{ GM}. \quad (1)$$

Note that since A_p is dimensionless the scaled result is multiplied by 1 GM to yield LEE NO_x with unit giga moles (GM). Figure 1 (top) depicts the May–July average A_p index, Fig. 1 (bottom) shows LEE NO_x derived using Eq. (1) (black) and average annual LEE NO_x after R07 (red). The good agreement indicates that in the Southern Hemisphere the interannual variability of the downward transport in the polar vortex is small, so that almost all of the variability can be explained by the variations in geomagnetic activity.

In order to derive a flux of NO_x , excess NO_x densities need to be considered. Similar

Title Page

Abstract

Introduction

Conclusions

References

Tables

Figures

◀

▶

◀

▶

Back

Close

Full Screen / Esc

Printer-friendly Version

Interactive Discussion



to above, the scaling function is derived using the data from R07 (their Fig. 7, reproduced here as Fig. 9). Then excess NO_x densities $g_{\text{LEE-NOX}}$ are

$$g_{\text{LEE-NOX}}(A_p) = A_p^{2.5} \cdot 2.20 \times 10^5 \text{ cm}^{-3}. \quad (2)$$

For the final flux calculation the following information are needed: (1) excess densities $g_{\text{LEE-NOX}}$, (2) an average vertical velocity, (3) a loss factor which accounts for transport out of the vortex as well as chemical loss. A value for the combination of the latter factors was established through a series of test simulations. For this, model $g_{\text{LEE-NOX}}$ at 45 km were compared to the results of R07 (their Fig. 7). The required flux was then determined to be

$$F = A_p^{2.5} \cdot c \cdot 2.20 \times 10^5 \text{ cm}^{-2} \text{ s}^{-1} \quad (3)$$

where $c=0.23$ for “average excess NO_x ” (see Fig. 9, or Fig. 7 of R07) and $c=0.45$ for “maximum excess NO_x ”. The transport to lower altitudes only acts at high latitudes during winter. Therefore, the flux needs to be constrained to a high-latitude region and be modulated as a function of time of the year. The following time dependency was chosen:

$$F = A_p^{2.5} \cdot c \cdot 2.20 \times 10^5 \text{ cm}^{-2} \text{ s}^{-1} \cdot \max(0.1, \cos(\pi/182.625 \cdot (d - 172.625))) \quad (4)$$

representing a sinusoidal flux centered around solstice. A restriction with respect to the latitudes where the flux is applied can be chosen via the namelist. There have been findings that enhancements occur down to 30–40° latitude (Siskind et al., 1997). However, Funke et al. (2005) showed that in the middle atmosphere the enhancements are confined to the vortex (their Figs. 5, 6, 7). Therefore we have here used a minimum absolute latitude of 55° representing a conservative estimate. The extent can be controlled via the namelist. Also possible would be a geomagnetic activity dependent latitudinal extent which has been suggested in the past, but because of other uncertainties this is not likely to improve the results significantly.

Here, the flux F is calculated from monthly mean values of A_p . The estimated flux is distributed in the form of NO over the top two model levels in order to avoid strong

**EPP in EMAC, NO_x
downward transport**A. J. G. Baumgaertner
et al.

Title Page

Abstract

Introduction

Conclusions

References

Tables

Figures

◀

▶

◀

▶

Back

Close

Full Screen / Esc

Printer-friendly Version

Interactive Discussion



gradients and other undesired effects that could result from introducing the flux into only the top layer, which acts as a sponge layer in the model.

The scaling function given by Eq. (3) was developed on the basis of NO_x enhancements in the southern polar region, therefore the parameterization is valid primarily for the Southern Hemisphere. In the Northern Hemisphere, it has been shown that also dynamical variability is an important factor (e.g. Randall et al., 2006). Depending on the model top height, and if the model correctly captures downward transport variability in the Northern Hemisphere, the same parameterization is valid also in the Northern Hemisphere. For the 90 level setup of EMAC, which reaches up to approximately 0.01 hPa, the necessary conditions are likely to be fulfilled. Therefore, the same parameterization was applied in the Northern Hemisphere. The validity of this approach is discussed further in the following section.

It should be noted that measurements of stratospheric NO_x are only available for a limited number of years. The geomagnetic A_p index in comparison has been measured since 1932 and reconstructions are possible for even larger timescales (Nagovitsyn, 2006). Therefore, the fact that the presented parameterization only requires the A_p index as an input function, and is not relying on satellite measurements, is of great advantage for model simulations spanning several decades.

A method often used to prescribe boundary conditions for different types of gases is to nudge the tracer to a known mixing ratio. In principle, using HALOE data this method would have been feasible to implement. However, the described emission of the tracer is preferable in this case since all other internal processes that modify the tracer tendency are not affected.

3 Results and discussion

In order to evaluate the technique, an EMAC simulation covering the period October 2002 to November 2003 is discussed. The SPACENOX submodel was included using “maximum excess NO_x ” scaling as described above. First, the model results for

EPP in EMAC, NO_x downward transport

A. J. G. Baumgaertner
et al.

Title Page

Abstract

Introduction

Conclusions

References

Tables

Figures

◀

▶

◀

▶

Back

Close

Full Screen / Esc

Printer-friendly Version

Interactive Discussion



the geomagnetically very active Southern Hemisphere winter 2003 are described and subsequently compared to satellite based NO_x measurements.

Figure 2 depicts the simulated mixing ratios of NO_x south of 60°S during 2003. Strong enhancements with mixing ratios of more than 300 ppbv are evident in the mesosphere. They are related to the NO_x produced by the SPACENOX submodel due to the large A_p index during most of the southern winter 2003 (see Fig. 1). Also clearly distinguishable is a sudden enhancement at the end of October. This is related to the solar proton event and is discussed in the companion paper (Baumgaertner et al., 2008). The latitudinal extent of the NO_x enhancements is shown in Fig. 3 for November and February during the Northern Hemisphere winter 2002/03 and for June and August during the following Southern Hemisphere winter. Mixing ratios up to 100 ppbv are evident from the north pole to 70°N , small enhancements are found as far as 40°N . Below the stratopause only small enhancements are found in both November and February, when polar winter downward transport would be expected to be effective. Any additional NO_x is confined to high latitudes. In June, in the Southern Hemisphere, mixing ratios of more than 200 ppbv extend to 60°S . In the upper stratosphere in August, NO_x enhancements of up to 20 ppbv still reach 60°S . This indicates that NO_x is confined by the polar vortex and will be discussed in more detail below.

Polar stratospheric enhancements of NO_x due to downward transport from the upper atmosphere have been presented by Funke et al. (2005), hereafter referred to as F05, using data from the MIPAS instrument on board ENVISAT. F05 presents results for the Southern Hemisphere winter 2003. Since these measurements did not form a basis for the parameterization in any form, the comparison will be independent. In order to ease a comparison with F05, potential temperature was chosen as vertical coordinate. This also allowed a consistent transformation to equivalent latitude (Nash et al., 1996). Transformed onto an equivalent latitude, potential vorticity increases (decreases) monotonically towards the north (south) pole. This allows a simple determination of the position of a grid box with respect to the edge of the polar vortex. Averaging over regions of high equivalent latitude means only small regions of air out-

**EPP in EMAC, NO_x
downward transport**A. J. G. Baumgaertner
et al.

Title Page

Abstract

Introduction

Conclusions

References

Tables

Figures

◀

▶

◀

▶

Back

Close

Full Screen / Esc

Printer-friendly Version

Interactive Discussion



side of the vortex are included. In addition, the vortex edge was calculated from the potential vorticity gradient according to Nash et al. (1996). With this it was possible during every model output timestep to determine the tracer average mixing ratio inside the polar vortex.

5 NO_x mixing ratios inside the polar vortex are shown in Fig. 4. Geopotential height was converted to an approximate geometric altitude and is shown in red contours. In Fig. 5 the corresponding MIPAS results of F05 are reproduced in order to ease a comparison. From the model results in Fig. 4 the downward transport of a NO_x enhancement exceeding 50 ppbv is clearly discernable and is in excellent agreement
10 with the MIPAS observations (Fig. 5) with respect to magnitude, timing, and altitude of the enhancements.

F05 also present measurements from the Northern Hemisphere winter 2002/2003. NO_2 nighttime abundances as a function of equivalent latitude and potential temperature are depicted in their Fig. 12 (top) and are reproduced here as Fig. 7. NO_2 enhancements last from November to February, interrupted by stratospheric warmings. They clearly result from downward transport and reach peak mixing ratios of 16 ppbv. EMAC NO_x mixing ratios for the same period are shown in Fig. 6. A strong downdraft of NO_2 appears at 3000 K in November, with mixing ratios of more than 16 ppbv. At
15 3000 K the enhancements last until February. The excess NO_2 is clearly transported down to altitudes of 1500 K (40 km). These results are also in excellent agreement with F05. This shows that the parameterization also works very well under moderate geomagnetic activity conditions and in the Northern Hemisphere. Note that the lower altitude enhancements found from January onwards have been shown to be related to midlatitude air that was transported to higher latitudes (see F05), resulting in NO_2 mixing ratios of up to 10 ppbv that last at least until April 2003.
20

To assess the interannual variability of LEE NO_x , the model results from a simulation covering 1992 to 2003 are compared to the results from R07. Different to the comparison with MIPAS, the data are not independent since the parameterization was build upon this data. The data for October 2002 to November 2003 is the same as
25

EPP in EMAC, NO_x downward transportA. J. G. Baumgaertner et al.

[Title Page](#)[Abstract](#)[Introduction](#)[Conclusions](#)[References](#)[Tables](#)[Figures](#)[◀](#)[▶](#)[◀](#)[▶](#)[Back](#)[Close](#)[Full Screen / Esc](#)[Printer-friendly Version](#)[Interactive Discussion](#)

**EPP in EMAC, NO_x
downward transport**A. J. G. Baumgaertner
et al.[Title Page](#)[Abstract](#)[Introduction](#)[Conclusions](#)[References](#)[Tables](#)[Figures](#)[◀](#)[▶](#)[◀](#)[▶](#)[Back](#)[Close](#)[Full Screen / Esc](#)[Printer-friendly Version](#)[Interactive Discussion](#)

discussed above, however, for 1992 to September 2002 the “average excess NO_x” scaling (see Sect. 2.2) was applied. Therefore, only half of the amount of NO_x was emitted into the model top. Figure 7 of R07, reproduced here as Fig. 9, shows excess NO_x densities at 45 km derived from HALOE data for 1992 to 2005 in 2-week time periods. Since HALOE derived densities in R07 ideally represent estimates for the entire vortex region, we have not sampled the model output at HALOE measurement locations. Instead NO_x densities were averaged over the area of the polar vortex and averaged in 2-week time periods in accordance with R07. In order to approximate excess densities, $0.75 \times 10^8 \text{ cm}^{-3}$ was subtracted from the absolute densities, which yielded almost no excess NO_x in the years where none is expected due to very low geomagnetic activity. The resulting EMAC excess densities are depicted in Fig. 8. Large interannual variability is evident. Almost no excess NO_x is seen in the years 1993, 1997, and 1999, while large amounts are found in 1994, 2000, and 2003. This is in agreement with the May–July A_p -index (Fig. 1), as expected. There is also a qualitative agreement with excess densities shown in Fig. 9 (or Fig. 7 from R07). In a number of years, quantitative agreement is also good. In 2003 maximum excess densities of up to $7 \times 10^8 \text{ cm}^{-3}$ were derived in R07, where the model shows between 6 and approximately $9 \times 10^8 \text{ cm}^{-3}$. Therefore, in 2003 there is good agreement with the maximum excess densities from R07. In the other years, when the “average excess NO_x” scaling was applied, the model agrees better with the average excess densities from R07. However, R07 considered the results based on the maximum excess densities more reasonable. In the light of the good agreement between MIPAS NO_x and the model simulation for 2003 with the “maximum excess NO_x” scaling, this conclusion by R07 is further corroborated.

Concerning a comparison of the temporal behavior of the model excess densities with the results shown in Fig. 9 (or Fig. 7 from R07), systematic discrepancies are found. As evident for example in the year 1995, elevated levels of NO_x density in R07 are found until early August, whereas model densities are usually only elevated until early July. There are several possibilities to explain these differing behaviors. Firstly, in

the model we prescribed a temporal behavior using a cosine function of time of the year, centered on solstice as described above. This means that statistically NO_x production is largest in June. However, due to the power-law dependency, this is unlikely to be the cause for the large fall-off after the end of June. For example, in 1995, this is clearly attributable to the change in A_p index: In May (June, July, August) the average A_p index was 18.6 (10.2, 7.7, 9.4). Another possible explanation lies in the HALOE sampling as a function of latitude. Until July HALOE measures only up to approx. 50°S , so it only captures NO_x enhancements near the vortex edge and misses the much larger enhancements towards the pole, as discussed by R07. In late winter, the sampling includes latitudes up to 70°S and thus also captures larger NO_x , but at least in some years (e.g. 1995) the bulk of the NO_x enhancements has already been transported to lower altitudes. The convolution of these two aspects could lead to a distorted apparent temporal behavior, i.e. underestimate early winter enhancements and overestimate late winter enhancements, possibly leading to a relatively monotonous enhancement as seen in Fig. 9 (or Fig. 7 of R07) in 1995.

It is also noteworthy that depending on the spatial and temporal averaging, model NO_x densities vary largely. This is illustrated in Fig. 10 where density is shown as a function of time and altitude for 2003. If lower altitudes were included in Fig. 8, the enhancement would appear to last longer.

Some of the features evident in Fig. 8 are related to Solar Proton Events. For example, the sudden increase in NO_x density in July 2000 lead to densities up to $11 \times 10^8 \text{ cm}^{-3}$. It is interesting to note that the enhancement in R07 is only half as large. The Solar Proton Event parameterization is discussed in the companion paper, therefore such features are not discussed further in the present study.

Due to the fact that NO_x can engage in catalytic ozone destruction, in the stratosphere significant effects on ozone can be expected during winters with high geomagnetic activity. Therefore EMAC results for the year 2003, where large amounts of NO_x were transported into the southern polar region, are shown here. In Fig. 11 the change of ozone mixing ratio inside the polar vortex with respect to 1996, a year with low ge-

EPP in EMAC, NO_x downward transport

A. J. G. Baumgaertner et al.

Title Page

Abstract

Introduction

Conclusions

References

Tables

Figures

◀

▶

◀

▶

Back

Close

Full Screen / Esc

Printer-friendly Version

Interactive Discussion



omagnetic activity (Fig. 8), is depicted. Depletion of up to 40% follows the downward transport of NO_x as seen in Fig. 4. Since ozone depletion due to chemistry involving chlorofluorocarbons was similar in the two years (not shown) and occurs at lower altitudes, it is evident that the depletion seen here is due to LEE NO_x .

5 Other members of the NO_y family are likely to be affected by the NO_x enhancements. Stiller et al. (2005) provided MIPAS measurements of strong HNO_3 enhancements inside the polar vortex during the Southern Hemisphere winter of 2003. EMAC results for HNO_3 in the same period are smaller by more than one order of magnitude. Since the relevant gas-phase reactions are included in the
10 simulation (see supplement: <http://www.atmos-chem-phys-discuss.net/8/21201/2008/acpd-8-21201-2008-supplement.zip>), this indicates that the measured HNO_3 enhancements are likely to results from ion cluster reactions (for more details see Stiller et al., 2005, and the companion paper) that are currently not included in EMAC.

4 Conclusions

15 A parameterization of the production of NO_x in the thermosphere through LEE has been developed with the aim to be able to describe NO_x mixing ratios in the stratospheric polar vortex. The approach is based solely on monthly mean values of the A_p index, which has been shown to be a good proxy for Southern Hemisphere interannual variations of vortex NO_x mixing ratios. A scaling function was developed based
20 on published interannual variations of LEE NO_x derived from HALOE measurements. The technique allows to quantitatively capture measured NO_x enhancements in the stratosphere that are due to LEE precipitation in the thermosphere. The implementation in EMAC was evaluated against independent NO_x measurements by MIPAS for the geomagnetically very active Southern Hemisphere winter 2003 as well as the moderately active Northern Hemisphere winter 2002/03. Excellent agreement was found for
25 both winters. For the Southern Hemisphere winter 2003 a significant impact on ozone was shown. The presented parameterization of LEE NO_x is therefore a valuable ad-

EPP in EMAC, NO_x downward transport

A. J. G. Baumgaertner
et al.

Title Page

Abstract

Introduction

Conclusions

References

Tables

Figures

◀

▶

◀

▶

Back

Close

Full Screen / Esc

Printer-friendly Version

Interactive Discussion



dition to the EMAC AC-GCM and will be useful for simulations of the recent climate. Because the A_p index is available since 1932, it is possible to quantify interannual variability on timescales even longer than satellite measurements of NO_x enhancements due to LEE. Combined with model implementations of other solar activity dependent processes, namely photolysis, radiative heating, and SPEs, it will be possible to study the holistic impact of solar activity variations on the earth's atmosphere. Results from an EMAC simulation encompassing these processes and covering the period 1960 until 2003 are in preparation for publication. Due to the success of the technique seen in the presented evaluation and its proven significance on polar ozone chemistry, it is recommended to include such a parameterization into middle atmosphere AC-GCMs.

Acknowledgements. This research was funded by the ProSECCO project within the DFG SPP 1176 CAUSES. We explicitly acknowledge the work by Randall et al. (2007) which laid the basis for the present study. We thank AGU as well as C. Randall and B. Funke for their kind permission to reproduce figures from their publications. We thank B. Funke for helpful comments on the manuscript. The Ferret program (<http://www.ferret.noaa.gov>) from NOAA's Pacific Marine Environmental Laboratory was used for creating some of the graphics in this paper. Thanks go to all MESSy developers and users for their support.



MAX-PLANCK-GESELLSCHAFT

The publication of this article is
financed by the Max Planck Society.

References

- Baumgaertner, A. J. G., Jöckel, P., Brühl, Ch., Stiller, G., and Funke, B.: Energetic particle precipitation in ECHAM5/MESSy1, Part 2: Solar proton events, Atmos. Chem. Phys. Discuss., in preparation, 2008. 21205, 21209
- Brühl, C., Steil, B., Stiller, G., Funke, B., and Jöckel, P.: Nitrogen compounds and ozone in the stratosphere: comparison of MIPAS satellite data with the chemistry climate model

21214

ACPD

8, 21201–21228, 2008

EPP in EMAC, NO_x downward transport

A. J. G. Baumgaertner
et al.

Title Page

Abstract

Introduction

Conclusions

References

Tables

Figures

◀

▶

◀

▶

Back

Close

Full Screen / Esc

Printer-friendly Version

Interactive Discussion



ECHAM5/MESSy1, *Atmos. Chem. Phys.*, 7, 5585–5598, 2007,

<http://www.atmos-chem-phys.net/7/5585/2007/>. 21205

Funke, B., López-Puertas, M., Gil-López, S., von Clarmann, T., Stiller, G. P., Fischer, H., and Kellmann, S.: Downward transport of upper atmospheric NO_x into the polar stratosphere and lower mesosphere during the Antarctic 2003 and Arctic 2002/2003 winters, *J. Geophys. Res.*, 110, D24308, doi:10.1029/2005JD006463, 2005. 21203, 21207, 21209, 21222, 21224

Hood, L. L. and Soukharev, B. E.: Solar induced variations of odd nitrogen: Multiple regression analysis of UARS HALOE data, *Geophys. Res. Lett.*, 33, L22805, doi:10.1029/2006GL028122, 2006. 21203, 21204

Jöckel, P., Tost, H., Pozzer, A., Brühl, C., Buchholz, J., Ganzeveld, L., Hoor, P., Kerweg, A., Lawrence, M. G., Sander, R., Steil, B., Stiller, G., Tanarhte, M., Taraborrelli, D., van Aardenne, J., and Lelieveld, J.: The atmospheric chemistry general circulation model ECHAM5/MESSy1: consistent simulation of ozone from the surface to the mesosphere, *Atmos. Chem. Phys.*, 6, 5067–5104, 2006,

<http://www.atmos-chem-phys.net/6/5067/2006/>. 21205

Langematz, U., Grenfell, J. L., Matthes, K., Mieth, P., Kunze, M., Steil, B., and Brühl, C.: Chemical effects in 11-year solar cycle simulations with the Freie Universität Berlin Climate Middle Atmosphere Model with online chemistry (FUB-CMAM-CHEM), *Geophys. Res. Lett.*, 32, L13803, doi:10.1029/2005GL022686, 2005. 21204

Lelieveld, J., Brühl, C., Jöckel, P., Steil, B., Crutzen, P. J., Fischer, H., Giorgetta, M. A., Hoor, P., Lawrence, M. G., Sausen, R., and Tost, H.: Stratospheric dryness: model simulations and satellite observations, *Atmos. Chem. Phys.*, 7, 1313–1332, 2007, <http://www.atmos-chem-phys.net/7/1313/2007/>. 21205

Mayaud, P. N.: Derivation, Meaning, and Use of Geomagnetic Indices, *Geophysical Monograph*, 22, Am. Geophys. Union, Washington DC, 1980. 21204

Nagovitsyn, Y. A.: Solar and geomagnetic activity on a long time scale: Reconstructions and possibilities for predictions, *Astron. Lett.*, 32, 344–352, doi:10.1134/S1063773706050082, 2006. 21208

Nash, E. R., Newman, P. A., Rosenfield, J. E., and Schoeberl, M. R.: An objective determination of the polar vortex using Ertel's potential vorticity, *J. Geophys. Res.*, 101, 9471–9478, 1996. 21209, 21210

Nissen, K. M., Matthes, K., Langematz, U., and Mayer, B.: Towards a better representation of the solar cycle in general circulation models, *Atmos. Chem. Phys.*, 7, 5391–5400, 2007,

ACPD

8, 21201–21228, 2008

EPP in EMAC, NO_x downward transport

A. J. G. Baumgaertner
et al.

Title Page

Abstract

Introduction

Conclusions

References

Tables

Figures

◀

▶

◀

▶

Back

Close

Full Screen / Esc

Printer-friendly Version

Interactive Discussion



**EPP in EMAC, NO_x
downward transport**A. J. G. Baumgaertner
et al.

<http://www.atmos-chem-phys.net/7/5391/2007/>. 21205

Randall, C. E., Rusch, D. W., Bevilacqua, R. M., Hoppel, K. W., and Lumpe, J. D.: Polar Ozone and Aerosol Measurement (POAM) II stratospheric NO₂, 1993–1996, *J. Geophys. Res.*, 103, 28 361–28 372, doi:10.1029/98JD02092, 1998. 21203, 21206

5 Randall, C. E., Harvey, V. L., Singleton, C. S., Bernath, P. F., Boone, C. D., and Kozyra, J. U.: Enhanced NO_x in 2006 linked to strong upper stratospheric Arctic vortex, *Geophys. Res. Lett.*, 33, L18811, doi:10.1029/2006GL027160, 2006. 21208

Randall, C. E., Harvey, V. L., Singleton, C. S., Bailey, S. M., Bernath, P. F., Codrescu, M., Nakajima, H., and Russell, J. M.: Energetic particle precipitation effects on the Southern Hemisphere stratosphere in 1992–2005, *J. Geophys. Res.*, 112, D08308, doi:10.1029/2006JD007696, 2007. 21203, 21204, 21206, 21214, 21226

10 Rinsland, C. P., Salawitch, R. J., Gunson, M. R., Solomon, S., Zander, R., Mahieu, E., Goldman, A., Newchurch, M. J., Irion, F. W., and Chang, A. Y.: Polar stratospheric descent of NO_y and CO and Arctic denitrification during winter 1992–1993, *J. Geophys. Res.*, 104, 1847–1861, doi:10.1029/1998JD100034, 1999. 21203

15 Roeckner, E., Brokopf, R., Esch, M., Giorgetta, M., Hagemann, S., Kornblueh, L., Manzini, E., Schlese, U., and Schulzweida, U.: Sensitivity of simulated climate to horizontal and vertical resolution in the ECHAM5 atmosphere model, *J. Climate*, 19, 3771, doi:10.1175/JCLI3824.1, 2006. 21205

20 Rozanov, E., Callis, L., Schlesinger, M., Yang, F., Andronova, N., and Zubov, V.: Atmospheric response to NO_y source due to energetic electron precipitation, *Geophys. Res. Lett.*, 32, L14811, doi:10.1029/2005GL023041, 2005. 21203

Rusch, D. W., Gérard, J.-C., Solomon, S., Crutzen, P. J., and Reid, G. C.: The effect of particle precipitation events on the neutral and ion chemistry of the middle atmosphere-I. Odd nitrogen, *Planet. Space Sci.*, 29, 767–774, doi:10.1016/0032-0633(81)90048-9, 1981. 21203

25 Russell, III, J. M., Rinsland, C. P., Farmer, C. B., Froidevaux, L., Toon, G. C., and Zander, R.: Measurements of odd nitrogen compounds in the stratosphere by the ATMOS experiment on Spacelab 3, *J. Geophys. Res.*, 93, 1718–1736, 1988. 21203

Sander, R., Kerkweg, A., Jöckel, P., and Lelieveld, J.: Technical Note: The new comprehensive atmospheric chemistry module MECCA, *Atmos. Chem. Phys.*, 5, 445–450, 2005, <http://www.atmos-chem-phys.net/5/445/2005/>. 21205

30 Seppälä, A., Clilverd, M. A., and Rodger, C. J.: NO_x enhancements in the middle atmosphere during 2003–2004 polar winter: Relative significance of solar proton events and the aurora

[Title Page](#)[Abstract](#)[Introduction](#)[Conclusions](#)[References](#)[Tables](#)[Figures](#)[◀](#)[▶](#)[◀](#)[▶](#)[Back](#)[Close](#)[Full Screen / Esc](#)[Printer-friendly Version](#)[Interactive Discussion](#)

- as a source, *J. Geophys. Res.*, 112, L23303, doi:10.1029/2006JD008326, 2007. 21203
- Siskind, D. E., Bacmeister, J. T., Summers, M. E., and Russell, III, J. M.: Two-dimensional model calculations of nitric oxide transport in the middle atmosphere and comparison with Halogen Occultation Experiment data, *J. Geophys. Res.*, 102, 3527–3546, doi:10.1029/96JD02970, 1997. 21204, 21207
- 5 Siskind, E., Nedoluha, G. E., Randall, C. E., Fromm, M., and Russell III, M.: An assessment of Southern Hemisphere stratospheric NO_x enhancements due to transport from the upper atmosphere, *Geophys. Res. Lett.*, 27, 329–332, 2000. 21203, 21204, 21206
- 10 Stiller, G. P., Mengistu Tsidu, G., von Clarmann, T., Glatthor, N., Höpfner, M., Kellmann, S., Linden, A., Ruhnke, R., Fischer, H., López-Puertas, M., Funke, B., and Gil-López, S.: An enhanced HNO₃ second maximum in the Antarctic midwinter upper stratosphere 2003, *J. Geophys. Res.*, 110, 20303, doi:10.1029/2005JD006011, 2005. 21213
- 15 Vogel, B., Konopka, P., Groöß, J.-U., Müller, R., Funke, B., López-Puertas, M., Reddmann, T., Stiller, G., von Clarmann, T., and Riese, M.: Model simulations of stratospheric ozone loss caused by enhanced mesospheric NO_x during Arctic winter 2003/2004, *Atmos. Chem. Phys.*, 8, 5279–5293, 2008, <http://www.atmos-chem-phys.net/8/5279/2008/>. 21204

EPP in EMAC, NO_x downward transportA. J. G. Baumgaertner
et al.

Title Page

Abstract

Introduction

Conclusions

References

Tables

Figures

I◀

▶I

◀

▶

Back

Close

Full Screen / Esc

Printer-friendly Version

Interactive Discussion



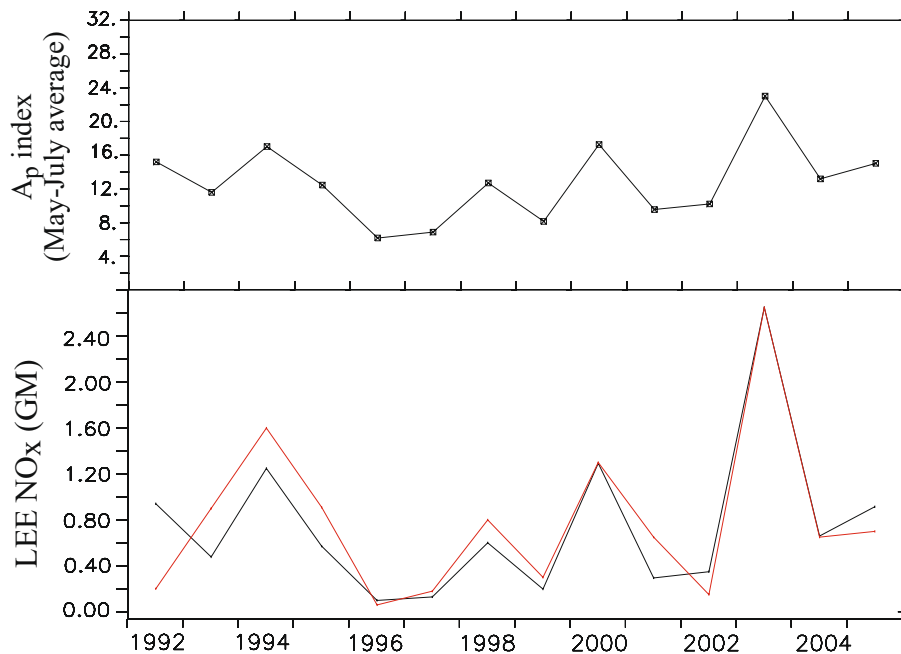
**EPP in EMAC, NO_x
downward transport**A. J. G. Baumgaertner
et al.

Fig. 1. Top: May–July average A_p index, bottom: LEE NO_x derived from the A_p index (black line) and maximum annual LEE NO_x after R07 (red line).

[Title Page](#)[Abstract](#)[Introduction](#)[Conclusions](#)[References](#)[Tables](#)[Figures](#)[◀](#)[▶](#)[◀](#)[▶](#)[Back](#)[Close](#)[Full Screen / Esc](#)[Printer-friendly Version](#)[Interactive Discussion](#)

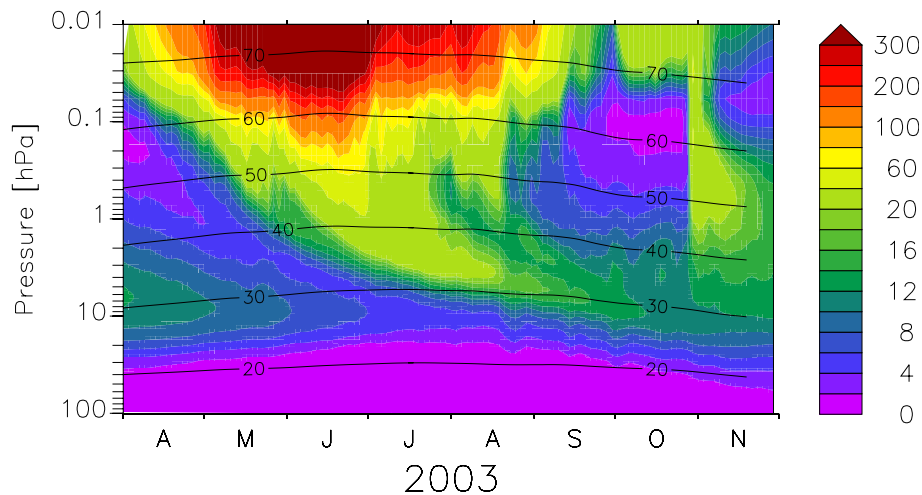
**EPP in EMAC, NO_x
downward transport**A. J. G. Baumgaertner
et al.

Fig. 2. EMAC NO_x mixing ratios (ppbv) averaged over 60°–90° S for 2003. The contour lines denote the altitude in km.

[Title Page](#)[Abstract](#)[Introduction](#)[Conclusions](#)[References](#)[Tables](#)[Figures](#)[◀](#)[▶](#)[◀](#)[▶](#)[Back](#)[Close](#)[Full Screen / Esc](#)[Printer-friendly Version](#)[Interactive Discussion](#)

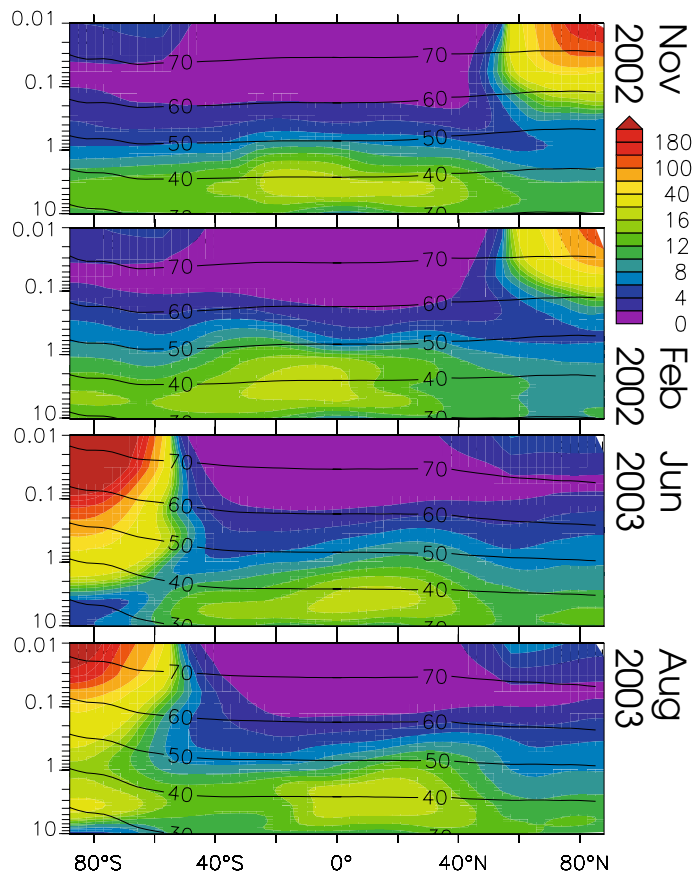
**EPP in EMAC, NO_x
downward transport**A. J. G. Baumgaertner
et al.

Fig. 3. EMAC NO_x mixing ratios (ppbv) as a function of latitude and pressure level for November and February 2002, and June and August 2003. The contour lines denote the corresponding altitude in km.

[Title Page](#)[Abstract](#)[Introduction](#)[Conclusions](#)[References](#)[Tables](#)[Figures](#)[◀](#)[▶](#)[◀](#)[▶](#)[Back](#)[Close](#)[Full Screen / Esc](#)[Printer-friendly Version](#)[Interactive Discussion](#)

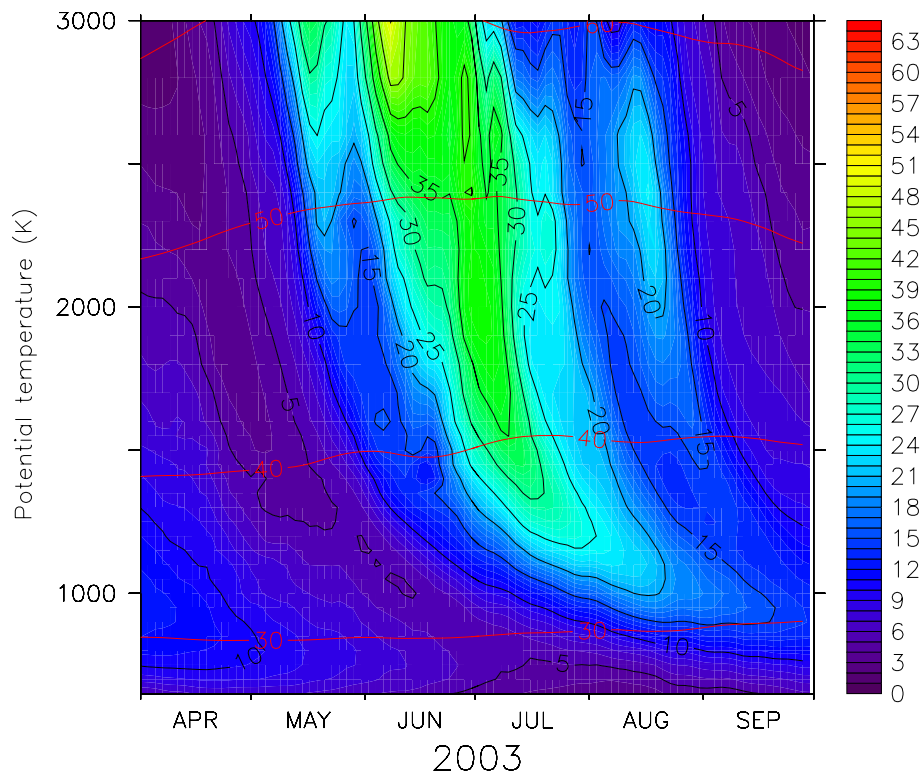
**EPP in EMAC, NO_x
downward transport**A. J. G. Baumgaertner
et al.

Fig. 4. EMAC NO_x mixing ratios (ppbv) inside the southern polar vortex during the Southern Hemisphere winter 2003. Red contours denote geometric altitudes in km.

[Title Page](#)[Abstract](#)[Introduction](#)[Conclusions](#)[References](#)[Tables](#)[Figures](#)[◀](#)[▶](#)[◀](#)[▶](#)[Back](#)[Close](#)[Full Screen / Esc](#)[Printer-friendly Version](#)[Interactive Discussion](#)

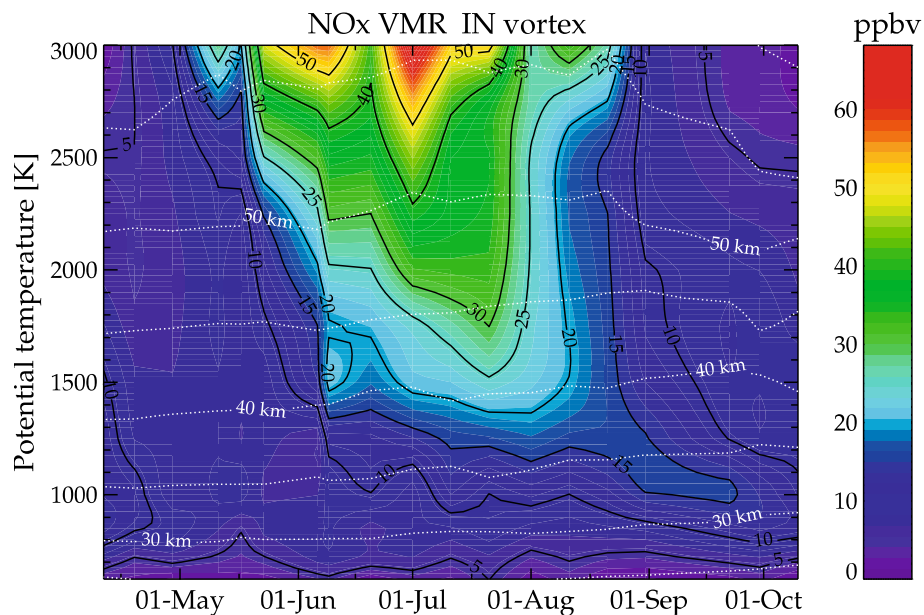
**EPP in EMAC, NO_x
downward transport**A. J. G. Baumgaertner
et al.

Fig. 5. NO_x mixing ratios inside the southern polar vortex measured by MIPAS (IMK/IAA data). Reproduced from Funke et al. (2005) with kind permission from AGU and B. Funke.

[Title Page](#)[Abstract](#)[Introduction](#)[Conclusions](#)[References](#)[Tables](#)[Figures](#)[◀](#)[▶](#)[◀](#)[▶](#)[Back](#)[Close](#)[Full Screen / Esc](#)[Printer-friendly Version](#)[Interactive Discussion](#)

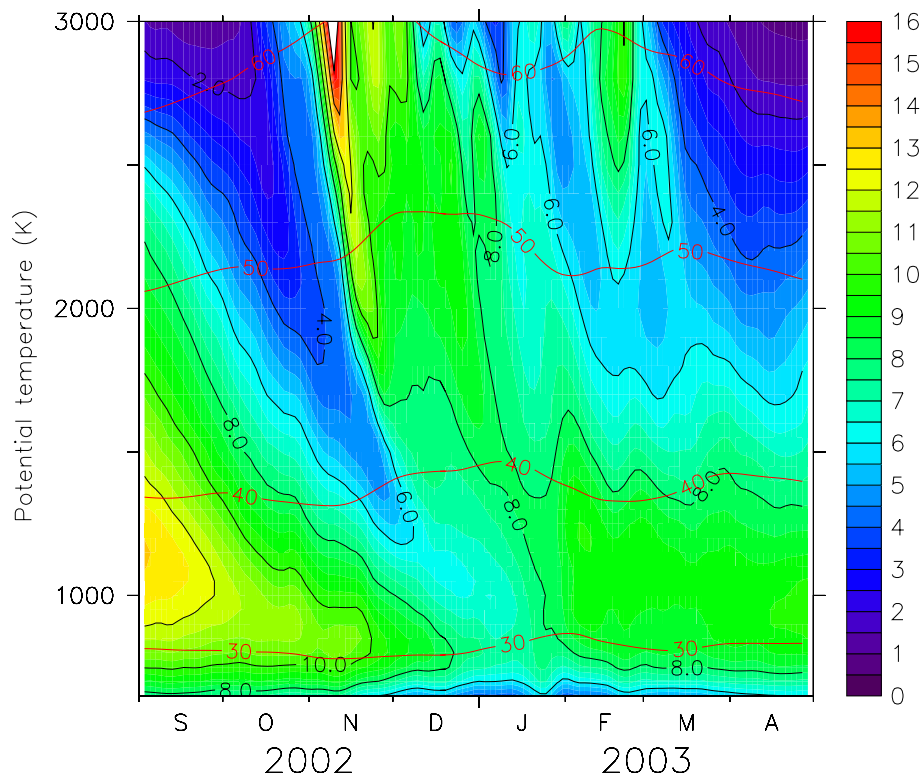
**EPP in EMAC, NO_x
downward transport**A. J. G. Baumgaertner
et al.

Fig. 6. EMAC NO_x mixing ratios (ppbv) averaged over 60°–90° N equivalent latitude during 2002/2003. The red lines denote geometric altitudes in km.

[Title Page](#)[Abstract](#)[Introduction](#)[Conclusions](#)[References](#)[Tables](#)[Figures](#)[◀](#)[▶](#)[◀](#)[▶](#)[Back](#)[Close](#)[Full Screen / Esc](#)[Printer-friendly Version](#)[Interactive Discussion](#)

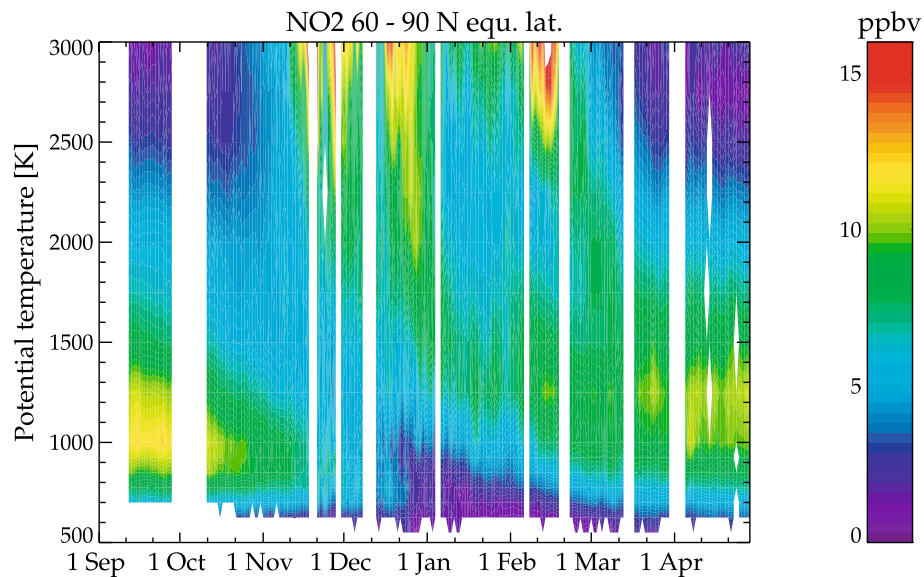
**EPP in EMAC, NO_x
downward transport**A. J. G. Baumgaertner
et al.

Fig. 7. Nighttime NO₂ mixing ratios measured by MIPAS (ESA data) averaged over 60°–90° N equivalent latitude. Reproduced from Funke et al. (2005) with kind permission from AGU and B. Funke.

[Title Page](#)[Abstract](#)[Introduction](#)[Conclusions](#)[References](#)[Tables](#)[Figures](#)[◀](#)[▶](#)[◀](#)[▶](#)[Back](#)[Close](#)[Full Screen / Esc](#)[Printer-friendly Version](#)[Interactive Discussion](#)

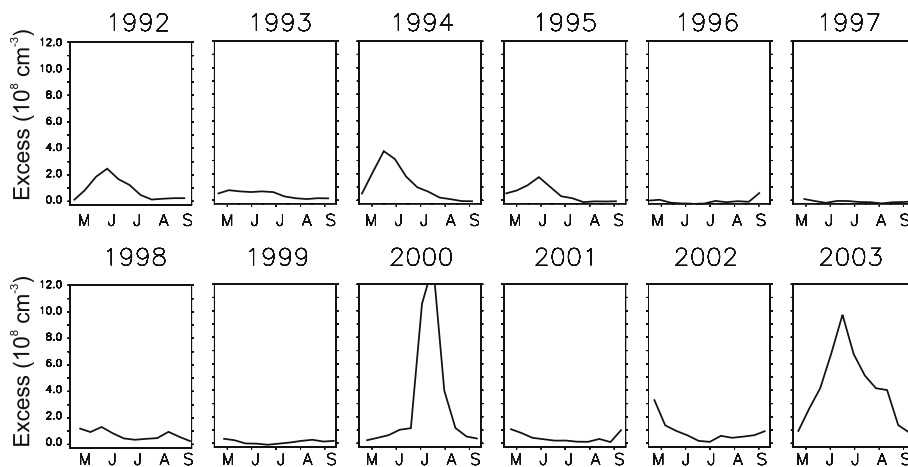
**EPP in EMAC, NO_x
downward transport**A. J. G. Baumgaertner
et al.

Fig. 8. EMAC excess NO_x densities inside the Southern Hemisphere polar vortex at 45 km. Note that for 1992–2002 the “average excess NO_x” scaling was applied, in 2003 the “maximum excess NO_x” scaling.

[Title Page](#)[Abstract](#)[Introduction](#)[Conclusions](#)[References](#)[Tables](#)[Figures](#)[◀](#)[▶](#)[◀](#)[▶](#)[Back](#)[Close](#)[Full Screen / Esc](#)[Printer-friendly Version](#)[Interactive Discussion](#)

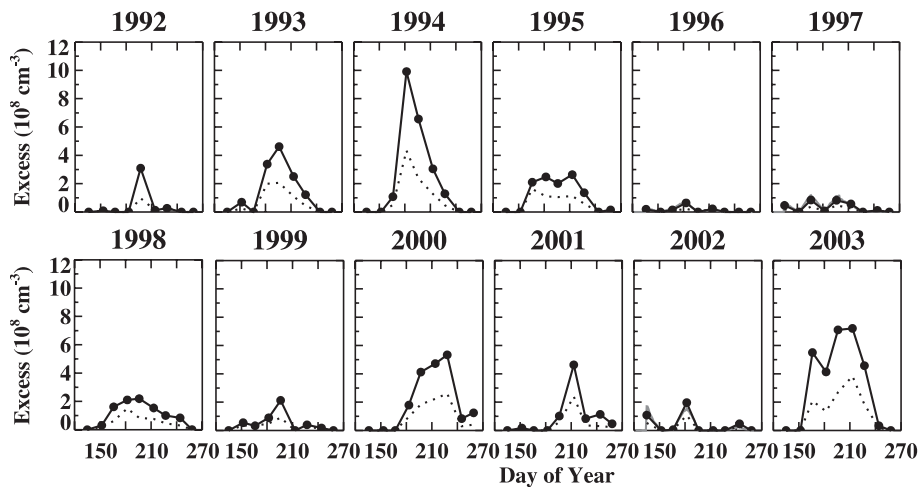
**EPP in EMAC, NO_x
downward transport**A. J. G. Baumgaertner
et al.

Fig. 9. Maximum (solid) and average (dotted) excess NO_x densities derived from HALOE. Reproduced from Randall et al. (2007) with kind permission from AGU and C. Randall.

[Title Page](#)[Abstract](#)[Introduction](#)[Conclusions](#)[References](#)[Tables](#)[Figures](#)[◀](#)[▶](#)[◀](#)[▶](#)[Back](#)[Close](#)[Full Screen / Esc](#)[Printer-friendly Version](#)[Interactive Discussion](#)

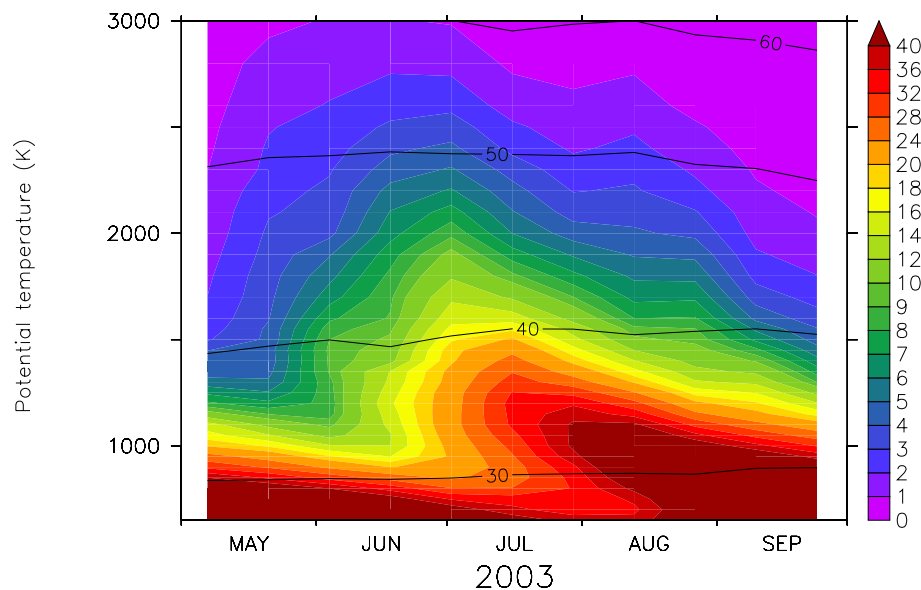
**EPP in EMAC, NO_x
downward transport**A. J. G. Baumgaertner
et al.

Fig. 10. EMAC excess NO_x densities (10^8 cm^{-3}) inside the southern polar vortex. The contours denote the approximate altitude in km.

[Title Page](#)[Abstract](#)[Introduction](#)[Conclusions](#)[References](#)[Tables](#)[Figures](#)[◀](#)[▶](#)[◀](#)[▶](#)[Back](#)[Close](#)[Full Screen / Esc](#)[Printer-friendly Version](#)[Interactive Discussion](#)

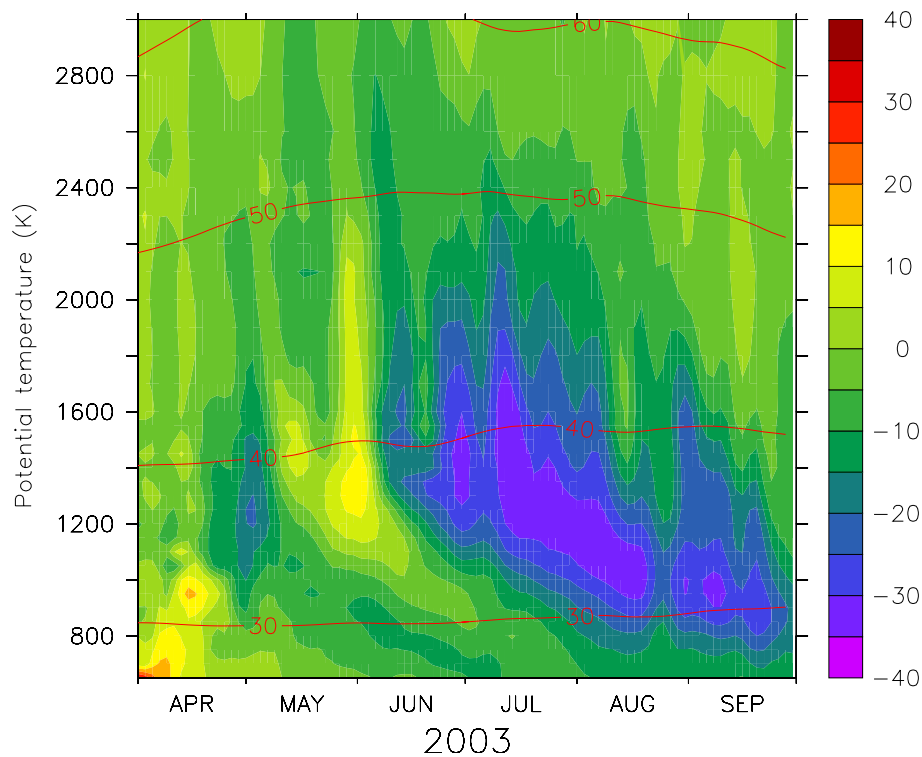
**EPP in EMAC, NO_x
downward transport**A. J. G. Baumgaertner
et al.

Fig. 11. Ozone change in 2003 with respect to the year 1996 in percent inside the polar vortex. The contours denote the approximate altitude in km.

[Title Page](#)[Abstract](#)[Introduction](#)[Conclusions](#)[References](#)[Tables](#)[Figures](#)[◀](#)[▶](#)[◀](#)[▶](#)[Back](#)[Close](#)[Full Screen / Esc](#)[Printer-friendly Version](#)[Interactive Discussion](#)